JVI Accepts, published online ahead of print on 13 August 2014
J. Virol. doi:10.1128/JVI.01215-14

Title: Type I interferon protects mice from fatal neurotropic infection with Langat virus by systemic and local anti-viral response

Elvira Weber[a,*,#], Katja Finsterbusch[b,*,##], Richard Lindquist[a], Sharmila Nair[b], Stefan Lienenklaus[c], Nelson O Gekara[d], Dirk Janik[e], Siegfried Weiss[c], Ulrich Kalinke[f], Anna K. Överby[a,¶] and Andrea Kröger[b,¶]

[a]Department of Clinical Microbiology, Virology, Umeå University, SE-901 85 Umeå, Sweden
[b]Innate Immunity and Infection; Helmholtz Centre for Infection Research, Braunschweig, Germany
[c]Department of Molecular Immunology, Helmholtz Centre for Infection Research, Braunschweig, Germany
[d]Department of Molecular Biology, Umeå University, SE-901 87 Umeå, Sweden
[e]Institute of Pathology, Helmholtz Center Munich, Neuherberg, Germany
[f]Institute for Experimental Infection Research, TWINCORE, Hannover, Germany
[*,¶] these authors contributed equally to this work

Running title: Type I IFN protects from LGTV neuropathogenesis

Address correspondence to Andrea Kröger, andrea.kroeger@helmholtz-hzi.de, or Anna K Överby, anna.overby@climi.umu.se
Present address: # Elvira Weber, Life & Medical Sciences Institute (LIMES), University of Bonn; ## Katja Finsterbusch, Department of Dermatology, Cardiff University, School of Medicine, Cardiff, United Kingdom

Word count abstract: 185

27 Word count text: 5535

Abstract

Vector-borne flaviviruses such as tick-borne encephalitis virus (TBEV), West Nile virus and dengue virus cause millions of infections in humans. TBEV causes a broad range of pathological symptoms ranging from meningitis to severe encephalitis or even hemorrhagic fever with high mortality. Despite the availability of an effective vaccine, incidence of TBEV infections is increasing. Not much is known about the role of the innate immune system in the control of TBEV infections. Here, we show that the type I interferon (IFN) system is essential for protection against TBEV and Langat virus (LGTV) in mice. In the absence of a functional IFN system, mice rapidly develop neurological symptoms and succumb to LGTV and TBEV infections. Type I IFN system deficiency results in severe neuro-inflammation in LGTV-infected mice characterized by breakdown of the blood-brain barrier and infiltration of macrophages into the central nervous system (CNS). Using mice with tissue-specific IFN receptor deletions, we show that a coordinated activation of the type I IFN system in peripheral tissues as well as in the CNS is indispensable for viral control and protection against virus induced inflammation and fatal encephalitis.

Importance

The type I interferon (IFN) system is important to control viral infections, however, the interactions between tick-borne encephalitis virus (TBEV) and the type I IFN system is poorly characterized. TBEV causes severe infections in humans that are characterized by fever and debilitating encephalitis, which can progress to chronic illness or death. No treatment options are available. An improved understanding of antiviral innate immune responses is pivotal for the development of effective therapeutics. We show that type I IFN, an effector molecule of the innate immune system is responsible for the extended survival of TBEV and Langat virus (LGTV), an attenuated member of the TBE serogroup. IFN production and signaling appeared to be essential in two different phases during infection: first in the periphery, by reducing

systemic LGTV replication and spreading into the central nervous system (CNS). Secondly, the local IFN response in the CNS prevents virus-induced inflammation and the development of encephalitis.

Introduction:

Flaviviruses (family *Flaviviridae*) are widely distributed all over the world. Such arthropod-borne viruses (arboviruses) are responsible for millions of debilitating human infections annually. They include West Nile virus (WNV), Japanese encephalitis virus (JEV), dengue virus (serotypes 1-4, DENV), yellow fever virus and tick-borne encephalitis virus (TBEV). TBEV is medically the most important arbovirus in Europe and Russia. Despite the availability of an effective vaccine, the number of infections is increasing and currently accounts for up to 10,000 cases per year (1, 2). The clinical spectrum ranges from mild symptoms to severe encephalitis, meningitis, hemorrhagic fever, or chronic progressive forms of the disease (2). While mortality rates vary from 0.5 to 30 %, neurological sequelae can occur in 30-60 % of survivors (1, 3, 4). For unknown reasons, encephalitis severity increases with age (2). Moreover, TBEV strains from Siberia and the Far East seem to be more aggressive than strains from Central Europe (3). Many aspects of TBEV infection and pathogenesis remain unresolved, especially its interactions with the innate immune system, and particularly the IFN system.

It is known that the IFN system is important for viral control and can contribute to viral pathogenicity (5, 6). Induction of type I IFNs is triggered by recognition of viral signature molecules such as double stranded RNA (dsRNA) and by pattern recognition receptors (PRRs) such as the cytoplasmic retinoic acid induced gene-I (RIG-I) family or the membrane bound Toll-like receptors (TLRs) (7, 8). Activation of PRRs leads to signaling cascades resulting in the activation of IFN genes via transcriptional factors IFN regulatory factor 3 (IRF-3) and IRF-7 (9, 10). Upon secretion, IFNs signal in a paracrine and autocrine manner via the type I IFN receptor (IFNAR) present on virtually all host cells to trigger the induction of IFN-stimulated genes (ISGs), which mediate an anti-viral and immune modulatory activity (11-13). ISGs can interfere with viral entry, viral transcription, translation, genome replication, or exit from the cell in a virus-specific manner (14).

Although type I IFN signaling is generally recognized as an important component of anti-viral innate immunity, studies so far indicate that its role during vector-borne flavivirus infections is complex and varies from one type of infection to the other. For instance, whereas type I IFN response in DENV infections limits only initial viral replication, it has no impact on disease development and control of the virus from the central nervous system (CNS) (15, 16). In WNV infections, type I IFN response limits viral replication, protects neurons from cell death and shapes maturation of anti-viral T cells but is not able to protect mice from lethal encephalitis (17, 18). The induction and role of type I IFNs during TBEV infection is not well understood. Owing to its ability to replicate within vesicles induced by rearrangement of cellular endoplasmic reticulum (ER) membranes, TBEV is able to prevent cellular recognition by pattern recognition receptors (PRR). This delays IFN-β induction which may give the virus a head start (19, 20). Similar strategies have been shown for Japanese encephalitis virus.

Although *in vivo* induction of IFN by TBEV has previously been reported (21, 22), whether it plays a protective role and in which cell types or tissues has not been addressed. To investigate, we used the naturally attenuated Langat (LGTV) virus, which belongs to the TBEV serogroup, as a model for TBEV infections. LGTV shares 82-88 % amino acid identity with TBEV and has been tested as a successful candidate for a live-attenuated vaccine for TBEV. However, vaccination was abandoned during clinical trials because encephalitis occurred in approximately 1:10,000 of vaccine recipients (3).

By combining the use of mice with complete body deficiency in IFNAR as well as mice conditionally ablated in the type I IFN system in the periphery and CNS, respectively, we show that restriction of viral growth and protection against ensuing immunopathology is contingent on the intricate interplay of type I IFN system in the periphery as well as in the CNS.

Materials & Methods

Mice and viral infections

C57BL/6 (WT) mice were purchased from Harlan. IFNAR$^{-/-}$, IFN-β$^{-/-}$, IFN-β$^{+/\Delta luc}$, IFNAR$^{fl/fl}$CreERT$^{+/-}$ and IFNAR$^{fl/fl}$NesCre$^{+/-}$ (23) mice on C57BL/6 background were bred under specific pathogen-free conditions at the Helmholtz Centre for Infection Research. For tamoxifen treatment, 2 mg was dissolved in 100 µl ClinOleic (Baxter, Lessines, Belgium). The solution was administered twice to 6-8 week old mice by oral gavage. VSV, LGTV strain TP21 and TBEV strain Hypr 71 was propagated in Vero B4 cells. Titers were determined by plaque assays on Vero B4 cells (19). 6-12 week-old mice were intraperitoneally infected with the indicated plaque forming units (pfu) of LGTV or TBEV strain Hypr in 100 µl PBS. For intracranial infections, mice were anesthetized by intraperitoneal injection with a mixture of ketamine (100 µg/g body weight) and xylazine (5 µg/g body weight). Mice were injected with 10 or 10^2 pfu of LGTV in 20 µl PBS. Administration of VSV was performed as described previously (35). Mice which lost more than 20 % of their body weight were sacrificed and perfused with 10 ml of PBS. All animal experiments were performed according to the guidelines of the German Animal Welfare Law (AZ 33.9-42502-05-12A295). Experiments with TBEV strain Hypr were performed in the BSL-3 facility at the Helmholtz Center for Infection Research.

IFN-α ELISA and Luciferase assay

The amount of murine IFN-α in mouse serum was determined by enzyme-linked immunosorbent assay (ELISA) according to the manufacturer's instructions (PBL). For the luciferase assay, mouse organs were homogenized in 500 µl Reporter Lysis Buffer (Promega) using the FastPrep-24 (MP). Lysates were mixed with LARII (Promega) and measured in a luminometer (Berthold). For *in vivo* imaging, mice were injected intravenously with 150 mg/kg of D-luciferin in PBS (CaliperLS), anesthetized using Isofluran (Baxter) and

135 monitored using an IVIS 200 imaging system (CaliperLS). Photon flux was quantified using
136 the Living Image 3.2 software (CaliperLS).
137
138 *RNA extraction and real-time RT-PCR*
139 Perfused mouse organs were homogenized in Trizol reagent (Invitrogen) using Lysis Matrix
140 (Nordic Biolabs) and the tissue homogenizer FastPrep-24 (MP). The RNA was extracted
141 using the Nucleo-Spin RNA II kit (Macherey Nagel). Total RNA (500-1000 ng) was used to
142 synthesize cDNA with the QuantiTect Reverse Transcription Kit (Qiagen). Levels of mouse
143 GAPDH, IFN-β, IL-6 and TNFα mRNA were detected by validated QuantiTect primer assays
144 (Qiagen) and the KAPA SYBR FAST qPCR Kit using the 7900HT Fast-Real-time PCR
145 System (Applied Biosystems). Viral TBEV RNAs were detected by TaqMan probes for
146 TBEV (24) and the KAPA probe FAST qPCR kit. The results were normalized using the
147 housekeeping gene GAPDH and analyzed as fold change relative to RNA samples from mock
148 infected mice using the comparative CT method ($\Delta\Delta_{CT}$). The sensitivity of the LGTV assay is
149 10^4 copies.
150
151 *Immune cell analysis*
152 Mice were sacrificed at indicated time points and perfused with 25 ml PBS. Brains were
153 isolated and homogenized through a 40 µm cell strainer and digested with collagenase D
154 (Roche) at room temperature for one hour. Immune cells were separated by centrifugation on
155 a discontinuous 70-to-30 % Percoll gradient. Cells were stained with antibodies specific for
156 CD3, CD4, CD8, CD11b, CD11c and CD45 (BD). Analysis was performed on a BD LSRII
157 using BD FACSDiva and FlowJo software. To identify infected immune cells, splenocytes
158 from 2 to 3 spleens were isolated by homogenization through a 40 µm mesh. Cells were
159 stained with specific antibodies for CD3, B220, CD11c and F4/80 (BD) and sorted by a BD
160 FACS Aria-II.

161

162 *Bone marrow chimeras*

163 Bone marrow chimeras of WT and IFNAR$^{-/-}$ mice were generated using standard techniques.
164 Congenitally marked CD45.1 or CD45.2 WT mice and CD45.2-marked IFNAR$^{-/-}$ mice were
165 used to track the bone marrow reconstitution. Bone marrow cells were collected from the hind
166 leg bones of 4-6 week old CD45.2 IFNAR$^{-/-}$ mice, CD45.1 WT mice and CD45.2 WT mice.
167 6-8 week old recipient mice were irradiated with 950 rads (9,5 Gy) to achieve complete bone
168 marrow ablation. One day after irradiation, 1×10^7 cells were intravenously injected to each
169 mouse via the tail vein. Mice were fed with enrofloxacin (Baytril) for two weeks and allowed
170 to recover for 6-8 weeks. Reconstitution of mice was analyzed by FACS, and successfully
171 reconstituted mice, determined by the CD45 marker (BD) and >80 % reconstitution, were
172 infected intraperitoneally with LGTV.

173

174 *Immunohistochemistry*

175 Immunohistochemical analysis was performed on LGTV-infected or non-infected IFNAR
176 mice at different time points (n=3 per time point). Brains and spleens were removed after
177 cardiac perfusion with PBS followed by 4 % paraformaldehyde. Organs were fixed in 4 %
178 neutrally buffered formaldehyde for 24 to 48h, embedded in paraffin, cut into 3µm sections
179 and stained with hematoxylin-eosin. Sections were evaluated by light-microscopy blinded to
180 the experimental groups. Immunohistochemistry was performed on the same formalin fixed
181 and paraffin embedded specimen. After heat mediated antigen retrieval, the sections were
182 stained by double staining with antiNS5/NeuN, anti EP/GFAP and anti EP/IBA1 for the brain
183 sections. Additionally, single staining for EP and IBA1 was conducted. The following
184 antibodies were used: mouse anti-GFAP (Sigma, 1:500), mouse anti-NeuN (Milipore, 1:500),
185 rabbit anti-IBA1 (Synaptic System, 1:500), mouse anti-E protein (25) and chicken anti-NS5
186 protein (1:1600) (26).

187

188 *Blood-brain barrier*

189 The integrity of the blood-brain barrier was assessed by Evan´s blue dye exclusion test. WT
190 and IFNAR$^{-/-}$ mice were infected intraperitoneally with LGTV. Mice were intravenously
191 injected with 100 µl 2 % Evans blue (Sigma) in PBS. After 1 hour, animals were
192 transcardially perfused with 20 ml PBS and the brains were removed, photographed, weighed,
193 and homogenized in 50 % TCA. After 30 minutes incubation at room temperature, samples
194 were spun down and absorbance of supernatants was measured at 620 nm.

195

196 **Results**

197 ***Type I IFN protects mice from lethal LGTV infection.*** The role of type I IFNs in infections
198 with flaviviruses is variable (16, 18, 27). WT, IFN-$\beta^{-/-}$ or IFNAR$^{-/-}$ mice were infected
199 intraperitoneally with 10^4 pfu of LGTV (Figure 1A) to assess the role of type I IFN signaling
200 in defense against LGTV. IFNAR$^{-/-}$ mice were found to be highly susceptible to LGTV
201 infection, displaying 100 % mortality compared to 20 % mortality in WT. WT mice showed
202 no signs of illness with the exception of two moribund mice, which showed weight loss and
203 hind limp paralysis within the first 2 days before they died. This is in contrast to all the
204 IFNAR$^{-/-}$ mice that exhibited onset of clinical signs on day 3-4 post-infection, including
205 weight loss, paralysis, hunchback posture, lethargy and fur ruffling. All IFNAR$^{-/-}$ mice died
206 within a mean survival time of 5 days post-infection. Even a dose as low as 1 pfu was found
207 to be lethal to IFNAR$^{-/-}$ mice within 5 days, further emphasizing the importance of the type I
208 IFN system in the protection against LGTV (Figure 1B). However, all mice deficient in IFN-β
209 survived without any symptoms indicating that IFN-α is sufficient to protect mice against the
210 lethal outcome of LGTV infections.
211
212 ***LGTV induces type I IFN response in multiple tissues thus inhibiting viral replication and***
213 ***spreading into the brain.*** Next we investigated the kinetics of type I IFN induction by LGTV
214 *in vivo* and the organs/tissues involved. WT mice infected intraperitoneally with 10^4 pfu of
215 LGTV had a significant IFN-α response at day 2 post-infection before returning to
216 background levels by day 4 (Figure 2A). Probably much like TBEV, which hides its dsRNA
217 from cytoplasmic PRR by rearranging internal ER-derived membranes thereby evading
218 detection by PRR pathways for IFN induction (19), IFN-α response elicited by LGTV was
219 much lower than that by Vesicular stomatitis virus (VSV), a member of the *Rhabdoviridae*
220 family, and a commonly used model for neurotropic viral infections. To complement the IFN-
221 α data and to determine the localization and kinetics of type I IFN induction, we took

advantage of a luciferase-based IFN-β reporter mouse strain IFN-$\beta^{+/\Delta\beta\text{-luc}}$, to image whole body IFN-β induction *in vivo* (28). Although the magnitude of IFN-β induction by LGTV was much lower than that by VSV, the response of IFN-β induction by both viruses *in vivo* was similar, peaking after 1 day, then declining to basal level by day 8 post-infection (Figure 2B/C). IFN-β induction by both viruses was localized to the thorax, peritoneum and inguinal lymph nodes 24 hours post-infection. At 48 hours post-infection, the signal was focused in the salivary gland region while 72 hours post-infection, it was mainly localized in the snout. This pattern of IFN-β induction was irrespective of infection doses (Figure 2B). Organ isolation and quantification of luciferase activity revealed that the peak IFN-β response within the first 24 hours, was mainly in lymphoid organs like lymph nodes, spleen and thymus and not liver, heart or lung (Figure 2D). Further analysis revealed cervical lymph nodes as the prominent source of the IFN-β response during this period. However, at later time points (e.g. 4 days post–infection) IFN-β responses could also be detected in the brain (Figure 2D). These results suggest that, peripheral inoculation of LGTV leads to type I IFN induction in multiple organs including lymphoid tissues and brain. Importantly, because the predominant type I IFN response induced by LGTV is presumably due to its dsRNA produced during viral replication, these results also suggest that LGTV can target and replicate in different peripheral organs and in the brain. To directly test this and evaluate if observed susceptibility of $IFNAR^{-/-}$ mice was due to uncontrolled viral replication, the viral load in different peripheral organs and central nervous system from WT and $IFNAR^{-/-}$ mice was calculated by real-time RT-PCR and determination of infectious particles by plaque assay. High infection doses are lethal in $IFNAR^{-/-}$ mice and since the kinetics of IFN-β induction is similar to low viral doses (Figure 2B), we performed the following experiments with a dose of 10^2 pfu. Consistent with the observed resistance to LGTV infection, viral RNA in peripheral organs and the central nervous system of WT mice was below the detection limit of our real time RT-PCR and no

247 viral particles were detectable by plaque assay (Figure 3). This is in contrast to IFNAR$^{-/-}$ mice
248 where viral RNA and infectious particles could readily be detected in peripheral organs (liver,
249 lung, spleen, kidney, thymus, lymph nodes), spinal cord and brain. In such mice, viral RNA
250 was observed to increase over time (Figure 3 and data not shown), indicating that ablation of
251 the type I IFN system results in unrestrained systemic viral replication. Importantly, the fact
252 that the virus was already detectable at 2 days post-infection indicates that the high
253 neuropathogenesis in LGTV-infected IFNAR$^{-/-}$ mice is due to rapid replication and spreading
254 of the virus into the brain (Figure 3B). In summary, the above results indicate that type I IFN
255 is crucial for protecting the animals from fatal outcome of infection both by restricting viral
256 replication in peripheral organs and its dissemination into the CNS.
257
258 ***Macrophages, dendritic cells and B220^{+} cells are the main targets of LGTV in lymphoid***
259 ***organs.*** The observations that IFN-β response and viral replication is mainly localized in
260 lymphoid organs such as the spleen (Figure 2B/C) prompted us to investigate the cell types
261 targeted by LGTV and the impact thereof on the lymphoid structure. Hematoxylin and eosin
262 (H&E) staining of the spleen at day 4 post-infection revealed hyperplasia of the red pulp,
263 severe depletion of lymphoid follicles, massive apoptosis, and histiocytic hyperplasia (Figure
264 4A). Sorting of splenocytes by flow cytometry harvested at different time points, followed by
265 analysis using real-time RT-PCR failed to detect viral RNA in B220^{+}, CD3^{+}, F4/80^{+} and
266 CD11c^{+} cells from infected WT mice (data not shown). This was in contrast to infected
267 IFNAR$^{-/-}$ mice where a time dependent increase in viral RNA was noted in F4/80^{+}, CD11c^{+}
268 cells and to some extent in B220^{+} cells (Figure 4C).
269
270 ***Type I IFN signaling in both hematopoietic and non-hematopoietic cells is indispensable***
271 ***for protection against LGTV infection.*** Beyond the hematopoietic (i.e. myeloid and
272 lymphoid) cells which - as shown above - are infected, next we sought to determine the

involvement of stromal cells. Towards this end, we established chimeric mice by adoptively transferring bone marrow from WT and IFNAR$^{-/-}$ mice into lethally irradiated WT and IFNAR$^{-/-}$ mice, further referred to as: WT→WT, WT→ IFNAR$^{-/-}$, IFNAR$^{-/-}$→WT, IFNAR$^{-/-}$ →IFNAR$^{-/-}$ (donor→irradiated recipient). Only mice with >80 % reconstitution were used. WT mice were more resistant to LGTV infection than WT→ WT bone marrow chimeras which could be due to side effects from the irradiation. In contrast to WT→ WT mice that were significantly more resistant to infection, both WT→ IFNAR$^{-/-}$ and IFNAR$^{-/-}$→ WT chimeras were unable to limit the infection and died within 5 to 6 days (Figure 5A). Curiously, although, no significant difference in survival was detected between WT→ IFNAR$^{-/-}$ and IFNAR$^{-/-}$→ WT chimeras, the viral load in the different organs (spleen, spinal cord and brain) of the chimera showed clear differences. IFNAR$^{-/-}$→ WT chimeras showed viral load in the spleen in the early stages (day 2 post-infection) but not later stages (day 4 post-infection) of infection. On the other hand, WT→ IFNAR$^{-/-}$ exhibited the highest viral load in the initial stages of infection (Figure 5B). The ability of WT hematopoietic cells to restrict viral growth in spleens of IFNAR$^{-/-}$ mice, mainly in the late stages suggests that in the spleen, initial infection and viral replication occurs in stromal cells and later in hematopoietic cells. This is in contrast to results seen in lungs, where IFNAR signaling in both hematopoietic and non-hematopoietic cells seemed to be crucial for controlling viral replication (Figure 5B). In the brain and spinal cord, viral RNA was detectable in mice lacking IFNAR on hematopoietic cells by day 2 post-infection. However, by day 4 post-infection, viral RNA was also detectable in the non-hematopoietic and partially radioresistent microglia of IFNAR$^{-/-}$ mice. Collectively, this data suggests that both hematopoietic and non-hematopoietic cells are targets of LGTV and that a coordinated type I IFN response in peripheral immune cells as well as brain cells is vital for viral control.

Type I IFN response in the periphery and the central nervous system is critical for host survival during LGTV infection. Given that LGTV and TBEV are neurotropic viruses that cause encephalitis, next we sought to investigate the impact of type I IFN signaling in direct anti-viral response in the CNS by administering the virus intracranially. Compared to the WT, $IFNAR^{-/-}$ mice were found to be highly susceptible to LGTV infections and died within 4 days post-infection with 10 pfu (Figure 6A). These results indicate that activation of type I IFN response in resident brain cells is essential for survival. For further investigation, we made use of two different transgenic animal models lacking the IFNAR in either the periphery or the CNS. The first is based on $IFNAR^{fl/fl}CreERT^{+/-}$ mice. Feeding twice with 2 mg of tamoxifen, the activation of Cre fused to the modified estrogen receptor (ERT) results in the deletion of IFNAR in the peripheral organs but not in the brain (Figure 6B). The second model is the $IFNAR^{fl/fl}NesCre^{+/-}$ mice where IFNAR is conditionally deleted in neuroectodermal cells of the CNS including neurons, oligodendrocytes and astrocytes but not microglia. Such mice show >90 % deletion efficiency in the brain, whereas other tissues such as spleen show no deletion (5, 23). Following intraperitoneal inoculation with 10^2 pfu of LGTV, all $IFNAR^{fl/fl}CreERT^{+/-}$mice developed severe clinical symptoms and died within 5 to 6 days (Figure 6B). $IFNAR^{fl/fl}NesCre^{+/-}$ mice did not show signs of disease until day 7, when they became hemiplegic and died within hours. This is in contrast to the $IFNAR^{fl/fl}$ mice fed with tamoxifen, which survived the infection (Figure 6B). A comparison of viral loads in lung and brain at a time point where both mice strains showed severe signs of illness; day 4 and day 8 for $IFNAR^{fl/fl}CreERT^{+/-}$ and $IFNAR^{fl/fl}NesCre^{+/-}$ respectively, revealed higher viral replication in lungs of $IFNAR^{fl/fl}CreERT^{+/-}$ (Figure 6C). Because no viral titers were detectable in the brain of $IFNAR^{fl/fl}CreERT^{+/-}$ mice, fatal infection of the CNS could not be the cause of death. On the other hand, $IFNAR^{fl/fl}NesCre^{+/-}$ displayed high viral replication in the brain on day 8 post-infection shortly before they died (Figure 6C). Consistent with an ability to target

different host cell types, this data suggests that a functional type I IFN system in the periphery as well as in the CNS is indispensable for restricting viral replication and entry into the brain. The primary target cells for LGTV replication in the brain are unknown. To strengthen the above findings, we performed immunohistochemical staining on different parts of the brain. No inflammatory response or lesions could be detected in the brain of infected IFNAR$^{-/-}$ mice by H&E staining (data not shown). Antibody staining against LGTV E protein detected several foci of virus infected cells mainly in the olfactory bulb, the medulla oblongata and to a minor extent in the brainstem and the cortexof IFNAR$^{-/-}$ but not WT mice (Figure 7A and data not shown). Cells of the meninges and choroid plexus were also strongly positive for LGTV. Further immunohistochemical analysis of the expression of the LGTV NS5 protein (brown) showed an association with NeuN^{+} neurons (red), whereas most of the GFAP^{+} astrocytes and IBA1^{+} microglia showed no sign of brown staining (Figure 7B). Thus, in the absence of IFNAR, LGTV spreads to different regions within the brain where it mainly infects neurons. This is comparable to VSV in which neurons are also infected (35).

IFNAR protects against inflammatory response in the brain. Given that LGTV-infected IFNAR$^{-/-}$ mice succumbed with symptoms of fatal encephalitis, next we characterized the inflammatory response within the brains of LGTV-infected mice by flow cytometry (Figure 7C). Whereas no T cells (CD3^{+}) were detectable in brains of WT or IFNAR$^{-/-}$ mice on day 4 post-infection, we observed infiltration of DCs (CD11c^{+}) and macrophages (CD45^{hi}CD11b^{+}), as well as an increase in activated microglia (CD45^{lo}CD11b^{+}). Importantly, the increased presence of macrophages and activated microglia was more pronounced in the CNS of IFNAR$^{-/-}$ mice (Figure 7C/D). Further analysis by real-time RT-PCR revealed a higher expression of the pro-inflammatory cytokines IL-6 and TNFα in the brain of infected IFNAR$^{-/-}$ mice (Figure 7E). Virus-induced neuroinflammation is often associated with the loss of blood-brain barrier (BBB) integrity (29). Evaluation of the integrity of the BBB by Evans blue

assay revealed a complete breakdown of the BBB allowing dye incorporation into brains of IFNAR$^{-/-}$ mice but not WT by 4 days post-infection (Figure 7F), an indication that type I IFNs are crucial for limiting viral replication and spreading into the CNS thereby preventing neuroinflammation and preserving the integrity of the BBB.

Type I IFN prolongs survival of TBEV-infected mice. To determine if type I IFNs also play an important role in highly pathogenic TBEV infections, we infected WT and IFNAR$^{-/-}$ mice with TBEV strain Hypr (Figure 8). Underscoring the importance of type I IFNs, TBEV-infected IFNAR$^{-/-}$ mice developed severe clinical symptoms including weight loss, paralysis, hunchback posture, lethargy and fur ruffling and died 5 days earlier than WT mice.

359 **Discussion**

360 Here we used LGTV, a naturally attenuated member of the TBEV serogroup, as a surrogate
361 pathogen to investigate the importance of type I IFN system in the course of TBEV infection.
362 Using mice with a defective IFN system we demonstrate the essential function of the type I
363 IFN system for the survival of the animal despite the fact that little IFN expression could be
364 detected in the serum by a reporter system. By using different knock-out mice, lacking type I
365 IFN response either in the periphery or the CNS, we showed that systemic type I IFN
366 response alone is not sufficient for viral control. Rather, the cooperation of peripheral and
367 local type I IFN response in the CNS is necessary to control viral replication and disease
368 progression.

369 The low amount of type I IFN induced by LGTV could be explained by inhibition of the IFN
370 system as a viral escape mechanism. We previously reported that TBEV rearranges
371 cytoplasmic membranes for the formation of virus factories and sequesters viral RNA in
372 membranous structures to hide them from detection by pathogen recognition receptors (19).
373 TBEV also antagonizes IFN signaling by impairment of IFN-stimulated JAK-STAT signal
374 transduction (30, 31). This leads to a reduced expression of anti-viral ISGs. Furthermore, anti-
375 viral responses can be dampened by interfering with a direct anti-viral response by TRIM79α,
376 which specifically inhibits TBEV replication (26) or by the inhibition of the positive feedback
377 loop of IFN induction by reduced IRF-7 expression (9). However, a specific protein
378 responsible for this inhibition by TBEV or LGTV has not yet been detected (19).

379 The general role of type I IFNs in *in vivo* infection with flaviviruses appears to be important.
380 Type I IFN is essential for controlling WNV infections, JEV and Murray Valley encephalitis
381 virus (18, 27, 32, 33). In contrast, $IFNAR^{-/-}$ mice showed no lethality following intravenous
382 infections with DENV, although viral replication and spread to some tissues is enhanced (16).
383 However, the suitability of the mouse model for this species-specific virus is debatable as the
384 viral evasion mechanism could be species–specific as well. Our experiments demonstrate that

385 although low amounts of type I IFN were produced upon LGTV infection, this amount is
386 sufficient to protect mice from fatal encephalitis. IFNAR$^{-/-}$ mice are highly susceptible to
387 LGTV infection and were unable to control the viral replication and spread. Interestingly, the
388 highly pathogenic TBEV strain Hypr showed the same phenotype as the attenuated LGTV in
389 IFNAR$^{-/-}$ mice, both strains killed the mice with the same kinetic, suggesting an important
390 role for the type I IFN system in reducing the infection progress of TBEV.
391 The type III IFNs seems to play a minor role in the CNS in response to viral infection
392 compared to type I IFNs. Only very low levels of IFN-λ mRNA have been detected in brains
393 of mice infected with mouse hepatitis virus or lactate dehydrogenase-elevating virus (LDV),
394 although IFN-λ was detectable in the liver (34). Various cell types of the CNS, including
395 oligodendrocytes, astrocytes and neurons respond to IFN produced upon viral infection.
396 While type I IFN receptor can be expressed by most cell types the type III IFN receptor
397 appears to be preferentially expressed by epithelial cells. However, very little is known about
398 the specific responsiveness of CNS cells to IFN-λ. Quantitative RT-PCR data show no
399 expression of the IFN-λ receptor, IL28R, in the CNS in contrast to lung tissue (35). However,
400 epithelial cells of the choroid plexus were infected by LGTV, so we cannot completely rule
401 out an IFN-λ mediated local antiviral effect in these cells.
402 The cellular tropism of LGTV is not completely understood. Intradermal injection followed
403 by *ex vivo* analysis revealed a primary infection of local dendritic cells, neutrophils and
404 monocytes (36). Furthermore, cell culture experiments showed that macrophages are
405 infectable and produce high amounts of viral titers (37). Our results *in vivo* show that LGTV
406 is indiscriminate and that it can target different hematopoietic and non-hematopoietic cell
407 types in the peripheral and CNS tissues. In the lymphoid tissues, LGTV mainly targets
408 macrophages, DCs, and B220^{+} cells as well as stromal cells, while in the CNS LGTV is found
409 distributed in several regions such olfactory bulb, medulla oblongata, brainstem and the
410 cortex. This broad cellular/tissue tropism may underlie the absolute requirement for a fully

411 functional type I IFN system in the peripheral tissues and CNS for halting viral replication
412 and disease pathology. In the case of DENV infections, type I IFN response limits only initial
413 viral replication but has no apparent effect on control of the virus from the CNS and disease
414 development (15, 16). Similarly, although important for controlling viral replication, type I
415 IFN response was not protective against lethal encephalitis during WNV infections (17, 18).
416 Whether the inherent differences in cellular tropism could explain the difference in the
417 requirement for type I IFNs during vector-borne flavivirus infections warrants further studies.
418 Irrespective of this, the broad cellular tropism of LGTV suggests that this virus is well
419 adapted to the murine system and thus more suitable for modeling neurotropic flavivirus
420 infection in mice.
421 The highest risk during neurotropic viral infection is the spread of the virus to the CNS
422 causing induction of inflammatory responses and the destruction of neuronal cells.
423 Immunopathology in TBEV infections is partly mediated by $CD8^+$ T cells and IFN-γ
424 production (38, 39), in which the antigen specificity rather than the number or activation level
425 of brain-infiltrating T cells is critical (40). The present study clearly shows no involvement of
426 T cells in the early state of infection but it does show that the type I IFN system plays an
427 essential role in preventing viral dissemination into the brain and its replication therein.
428 Precisely how the virus gains entry into the brain and which cell types are responsible in type
429 I IFN response in the CNS is unclear. Our IFN-β luciferase reporter mice show that LGTV
430 can induce IFN-β gene induction in the brain, an indication of viral replication therein. Since
431 such mice do not show any signs of disease, these observations alongside the fact that viral
432 RNA can be detected in $IFNAR^{fl/fl}NesCre^{+/-}$ mice in which IFNAR is only deleted in the CNS,
433 indicate that the virus enters the CNS despite the presence of a functional IFN system in the
434 periphery.
435 One of the possible mechanisms of viral entry into the brain is via recruitment of infected
436 inflammatory cells through the damaged BBB. However, this is unlikely the case for LGTV.

437 Since TBEV has previously been shown to enter the brain through the intact BBB (29). In
438 accordance, we could already detect LGTV RNA in the brain of IFNAR$^{-/-}$ mice by day 2 post-
439 infection, well before BBB breakdown which occurred at day 4. Furthermore, the IFN-β
440 response seen in the brains of IFN-β luciferase reporter mice which did not show signs of
441 neuroinflammation suggests that entry of LGTV into the brain is not due to breakdown of the
442 BBB. Increased BBB permeability corresponds to expression of several chemokines and
443 cytokines (41, 42). Accordingly, TNFα, IL-6 and Ccl5 mRNA was detectable in the brains of
444 infected IFNAR$^{-/-}$ mice. Thus, the BBB breakdown in LGTV infected mice is most likely due
445 to the inflammatory cytokines and chemokines induced by viral replication in the brain. A
446 more viable mechanism of viral entry into the brain could be via retrograde axonal
447 transportation of the virus from peripheral nerve cells, a mechanism which has previously
448 been shown for WNV (43) and enterovirus 71 (44).
449 In summary, type I IFN signaling plays a critical role in the host's defense against LGTV in
450 two distinct phases during infection: 1. in the periphery, by limiting systemic LGTV
451 replication and dissemination, which limits the amount of virus spread to the CNS. 2. Directly
452 in the CNS, by a local anti-viral response, which prevents virus induced inflammation and the
453 development of encephalitis.
454

Acknowledgments

Grant support: This work was supported by the Helmholtz International Research School for Infection Biology (HIRSIB) (A.K), the Graduate School of the Helmholtz Centre for Infection Research (K.F.; S.N.), the Kempe Foundations, the Laboratory for Molecular Medicine Sweden (MIMS), Umeå center for microbial research (UCMR) and Linneus support, the Jeanssons foundations and the Swedish foundation for international cooperation in research and higher education (STINT) (A.Ö).

We thank Martina Grashoff and Denise Fortuné for excellent technical assistance. Moreover, we thank Hansjörg Hauser for helpful discussion. Histological sections and stainings were done by Marina Pils of the mousepathology platform of the Helmholtz Centre for Infection Research.

References

1. **Charrel RN, Attoui H, Butenko AM, Clegg JC, Deubel V, Frolova TV, Gould EA, Gritsun TS, Heinz FX, Labuda M, Lashkevich VA, Loktev V, Lundkvist A, Lvov DV, Mandl CW, Niedrig M, Papa A, Petrov VS, Plyusnin A, Randolph S, Suss J, Zlobin VI, de Lamballerie X.** 2004. Tick-borne virus diseases of human interest in Europe. Clinical microbiology and infection : the official publication of the European Society of Clinical Microbiology and Infectious Diseases **10:**1040-1055.
2. **Lindquist L, Vapalahti O.** 2008. Tick-borne encephalitis. Lancet **371:**1861-1871.
3. **Gritsun TS, Lashkevich VA, Gould EA.** 2003. Tick-borne encephalitis. Antiviral research **57:**129-146.
4. **Heinz FX, Kunz C.** 2004. Tick-borne encephalitis and the impact of vaccination. Archives of virology. Supplementum**:**201-205.
5. **Detje CN, Meyer T, Schmidt H, Kreuz D, Rose JK, Bechmann I, Prinz M, Kalinke U.** 2009. Local type I IFN receptor signaling protects against virus spread within the central nervous system. Journal of immunology (Baltimore, Md. : 1950) **182:**2297-2304.
6. **Muller U, Steinhoff U, Reis LF, Hemmi S, Pavlovic J, Zinkernagel RM, Aguet M.** 1994. Functional role of type I and type II interferons in antiviral defense. Science (New York, N.Y.) **264:**1918-1921.
7. **Akira S, Uematsu S, Takeuchi O.** 2006. Pathogen recognition and innate immunity. Cell **124:**783-801.
8. **Yoneyama M, Kikuchi M, Natsukawa T, Shinobu N, Imaizumi T, Miyagishi M, Taira K, Akira S, Fujita T.** 2004. The RNA helicase RIG-I has an essential function in double-stranded RNA-induced innate antiviral responses. Nature immunology **5:**730-737.

9. **Marie I, Durbin JE, Levy DE.** 1998. Differential viral induction of distinct interferon-alpha genes by positive feedback through interferon regulatory factor-7. The EMBO journal **17:**6660-6669.

10. **Lin R, Heylbroeck C, Pitha PM, Hiscott J.** 1998. Virus-dependent phosphorylation of the IRF-3 transcription factor regulates nuclear translocation, transactivation potential, and proteasome-mediated degradation. Molecular and cellular biology **18:**2986-2996.

11. **Durbin JE, Hackenmiller R, Simon MC, Levy DE.** 1996. Targeted disruption of the mouse Stat1 gene results in compromised innate immunity to viral disease. Cell **84:**443-450.

12. **Farrar JD, Murphy KM.** 2000. Type I interferons and T helper development. Immunology today **21:**484-489.

13. **Der SD, Zhou A, Williams BR, Silverman RH.** 1998. Identification of genes differentially regulated by interferon alpha, beta, or gamma using oligonucleotide arrays. Proceedings of the National Academy of Sciences of the United States of America **95:**15623-15628.

14. **Schoggins JW, Wilson SJ, Panis M, Murphy MY, Jones CT, Bieniasz P, Rice CM.** 2011. A diverse range of gene products are effectors of the type I interferon antiviral response. Nature **472:**481-485.

15. **Prestwood TR, Morar MM, Zellweger RM, Miller R, May MM, Yauch LE, Lada SM, Shresta S.** 2012. Gamma interferon (IFN-gamma) receptor restricts systemic dengue virus replication and prevents paralysis in IFN-alpha/beta receptor-deficient mice. Journal of virology **86:**12561-12570.

16. **Shresta S, Kyle JL, Snider HM, Basavapatna M, Beatty PR, Harris E.** 2004. Interferon-dependent immunity is essential for resistance to primary dengue virus

infection in mice, whereas T- and B-cell-dependent immunity are less critical. Journal of virology **78:**2701-2710.

17. **Pinto AK, Daffis S, Brien JD, Gainey MD, Yokoyama WM, Sheehan KC, Murphy KM, Schreiber RD, Diamond MS.** 2011. A temporal role of type I interferon signaling in CD8+ T cell maturation during acute West Nile virus infection. PLoS pathogens **7:**e1002407.

18. **Samuel MA, Diamond MS.** 2005. Alpha/beta interferon protects against lethal West Nile virus infection by restricting cellular tropism and enhancing neuronal survival. Journal of virology **79:**13350-13361.

19. **Overby AK, Popov VL, Niedrig M, Weber F.** 2010. Tick-borne encephalitis virus delays interferon induction and hides its double-stranded RNA in intracellular membrane vesicles. Journal of virology **84:**8470-8483.

20. **Overby AK, Weber F.** 2011. Hiding from intracellular pattern recognition receptors, a passive strategy of flavivirus immune evasion. Virulence **2:**238-240.

21. **Kopecky J, Tomkova E, Vlcek M.** 1991. Immune response of the long-tailed field mouse (Apodemus sylvaticus) to tick-borne encephalitis virus infection. Folia parasitologica **38:**275-282.

22. **Baker DG, Woods TA, Butchi NB, Morgan TM, Taylor RT, Sunyakumthorn P, Mukherjee P, Lubick KJ, Best SM, Peterson KE.** 2013. Toll-like receptor 7 suppresses virus replication in neurons but does not affect viral pathogenesis in a mouse model of Langat virus infection. The Journal of general virology **94:**336-347.

23. **Prinz M, Schmidt H, Mildner A, Knobeloch KP, Hanisch UK, Raasch J, Merkler D, Detje C, Gutcher I, Mages J, Lang R, Martin R, Gold R, Becher B, Bruck W, Kalinke U.** 2008. Distinct and nonredundant in vivo functions of IFNAR on myeloid cells limit autoimmunity in the central nervous system. Immunity **28:**675-686.

24. **Schwaiger M, Cassinotti P.** 2003. Development of a quantitative real-time RT-PCR assay with internal control for the laboratory detection of tick borne encephalitis virus (TBEV) RNA. Journal of clinical virology : the official publication of the Pan American Society for Clinical Virology **27:**136-145.

25. **Niedrig M, Klockmann U, Lang W, Roeder J, Burk S, Modrow S, Pauli G.** 1994. Monoclonal antibodies directed against tick-borne encephalitis virus with neutralizing activity in vivo. Acta virologica **38:**141-149.

26. **Taylor RT, Lubick KJ, Robertson SJ, Broughton JP, Bloom ME, Bresnahan WA, Best SM.** 2011. TRIM79alpha, an interferon-stimulated gene product, restricts tick-borne encephalitis virus replication by degrading the viral RNA polymerase. Cell host & microbe **10:**185-196.

27. **Lobigs M, Mullbacher A, Wang Y, Pavy M, Lee E.** 2003. Role of type I and type II interferon responses in recovery from infection with an encephalitic flavivirus. The Journal of general virology **84:**567-572.

28. **Lienenklaus S, Cornitescu M, Zietara N, Lyszkiewicz M, Gekara N, Jablonska J, Edenhofer F, Rajewsky K, Bruder D, Hafner M, Staeheli P, Weiss S.** 2009. Novel reporter mouse reveals constitutive and inflammatory expression of IFN-beta in vivo. Journal of immunology (Baltimore, Md. : 1950) **183:**3229-3236.

29. **Ruzek D, Salat J, Singh SK, Kopecky J.** 2011. Breakdown of the blood-brain barrier during tick-borne encephalitis in mice is not dependent on CD8+ T-cells. PloS one **6:**e20472.

30. **Best SM, Morris KL, Shannon JG, Robertson SJ, Mitzel DN, Park GS, Boer E, Wolfinbarger JB, Bloom ME.** 2005. Inhibition of interferon-stimulated JAK-STAT signaling by a tick-borne flavivirus and identification of NS5 as an interferon antagonist. Journal of virology **79:**12828-12839.

31. **Werme K, Wigerius M, Johansson M.** 2008. Tick-borne encephalitis virus NS5 associates with membrane protein scribble and impairs interferon-stimulated JAK-STAT signalling. Cellular microbiology **10:**696-712.

32. **Lazear HM, Pinto AK, Vogt MR, Gale M, Jr., Diamond MS.** 2011. Beta interferon controls West Nile virus infection and pathogenesis in mice. Journal of virology **85:**7186-7194.

33. **Lee E, Lobigs M.** 2002. Mechanism of virulence attenuation of glycosaminoglycan-binding variants of Japanese encephalitis virus and Murray Valley encephalitis virus. Journal of virology **76:**4901-4911.

34. **Sommereyns C, Paul S, Staeheli P, Michiels T.** 2008. IFN-lambda (IFN-lambda) is expressed in a tissue-dependent fashion and primarily acts on epithelial cells in vivo. PLoS pathogens **4:**e1000017.

35. **Nair S, Michaelsen-Preusse K, Finsterbusch K, Stegemann-Koniszewski S, Bruder D, Grashoff M, Korte M, Koster M, Kalinke U, Hauser H, Kroger A.** 2014. Interferon regulatory factor-1 protects from fatal neurotropic infection with vesicular stomatitis virus by specific inhibition of viral replication in neurons. PLoS pathogens **10:**e1003999.

36. **Labuda M, Austyn JM, Zuffova E, Kozuch O, Fuchsberger N, Lysy J, Nuttall PA.** 1996. Importance of localized skin infection in tick-borne encephalitis virus transmission. Virology **219:**357-366.

37. **Ahantarig A, Ruzek D, Vancova M, Janowitz A, St'astna H, Tesarova M, Grubhoffer L.** 2009. Tick-borne encephalitis virus infection of cultured mouse macrophages. Intervirology **52:**283-290.

38. **Ruzek D, Salat J, Palus M, Gritsun TS, Gould EA, Dykova I, Skallova A, Jelinek J, Kopecky J, Grubhoffer L.** 2009. CD8+ T-cells mediate immunopathology in tick-borne encephalitis. Virology **384:**1-6.

593 39. **Palus M, Vojtiskova J, Salat J, Kopecky J, Grubhoffer L, Lipoldova M, Demant**
594 **P, Ruzek D.** 2013. Mice with different susceptibility to tick-borne encephalitis virus
595 infection show selective neutralizing antibody response and inflammatory reaction in
596 the central nervous system. Journal of neuroinflammation **10:**77.
597 40. **Fujii Y, Hayasaka D, Kitaura K, Takasaki T, Suzuki R, Kurane I.** 2011. T-cell
598 clones expressing different T-cell receptors accumulate in the brains of dying and
599 surviving mice after peripheral infection with far eastern strain of tick-borne
600 encephalitis virus. Viral immunology **24:**291-302.
601 41. **Abbott NJ.** 2000. Inflammatory mediators and modulation of blood-brain barrier
602 permeability. Cellular and molecular neurobiology **20:**131-147.
603 42. **de Vries HE, Blom-Roosemalen MC, van Oosten M, de Boer AG, van Berkel TJ,**
604 **Breimer DD, Kuiper J.** 1996. The influence of cytokines on the integrity of the
605 blood-brain barrier in vitro. Journal of neuroimmunology **64:**37-43.
606 43. **Samuel MA, Wang H, Siddharthan V, Morrey JD, Diamond MS.** 2007. Axonal
607 transport mediates West Nile virus entry into the central nervous system and induces
608 acute flaccid paralysis. Proceedings of the National Academy of Sciences of the
609 United States of America **104:**17140-17145.
610 44. **Chen CS, Yao YC, Lin SC, Lee YP, Wang YF, Wang JR, Liu CC, Lei HY, Yu**
611 **CK.** 2007. Retrograde axonal transport: a major transmission route of enterovirus 71
612 in mice. Journal of virology **81:**8996-9003.

613
614

615 **Figure Legends**

616 **Figure 1. Type I IFN response is crucial for survival of infections.**

617 A, Survival analysis of WT, IFNAR$^{-/-}$, and IFNβ$^{-/-}$ mice (n=10). 6-8 week old age-matched
618 mice were infected intraperitoneally with 10^4 pfu of LGTV, and mortality was observed for
619 21 days. B, Survival analysis of IFNAR$^{-/-}$ mice after intraperitoneal infection with 100, 10 and
620 1 pfu of LGTV (n=5). Data are cumulative of at least two independent experiments. Survival
621 differences were tested for statistical significance by the log-rank test.

622

623 **Figure 2. LGTV infection leads to type I IFN induction.**

624 A, Mice were infected intraperioneally with 10^4 pfu of LGTV or intranasally with 10^4 pfu
625 VSV. Serum was collected on day 0, 2 and 4 post-infection. IFN-α protein level was
626 determined by ELISA. B, Whole-body imaging of IFN-β$^{+/\Delta\beta\text{-luc}}$ reporter mice after
627 intraperitoneal infection with 10^2 and 10^4 pfu of LGTV. Mice were imaged before treatment
628 (0 h) and over time as indicated. Images from a representative mouse are shown. The rainbow
629 scale indicates the number of photons measured per second per cm^2 per steradian (sr). C,
630 Comparison of IFN-β induction in VSV and LGTV-infected mice. Mice were infected
631 intraperitoneally with 10^4 pfu of LGTV or intranasally with 10^4 pfu VSV. Whole-body
632 imaging of IFN-β$^{+/\Delta\beta\text{-luc}}$ reporter mice. Mice were imaged before treatment (0 h) and over time
633 as indicated; one representative mouse is shown. Images from LGTV-infected mice are
634 identical with that of figure 2B, but shown in another range of the rainbow scale to prevent
635 saturation of pictures from VSV-infected mice. The scale indicates the number of photons
636 measured per second per cm^2 per steradian (sr). D, Quantification of luciferase activity in
637 different organs of IFN-β$^{+/\Delta\beta\text{-luc}}$ mice. Mice were sacrificed at the indicated time points post-
638 infection and selected organs were isolated and homogenized for luciferase activity
639 measurement. Fold induction represents relative luminescence units per organ. LN, lymph

640 nodes. Data represent the mean ± SEM of 3 to 7 mice per time point from at least two
641 independent experiments. Asterisks indicate values that were statistically significant: **, P <
642 0.01, based on the Mann-Whitney test.
643
644 **Figure 3. Type I IFN limits LGTV replication and spread.**
645 WT and IFNAR$^{-/-}$ mice were infected intraperitoneally with 10^2 pfu of LGTV and viral load
646 was measured by real-time RT-PCR (A/B) and plaque forming units (C/D). Detection of
647 relative LGTV mRNA levels in spleen and lung (A), as well as spinal cord and brain (B) on
648 day 2 and 4 post-infection. Determination of viral particles in spleen and lung (C), as well as
649 spinal cord and brain (D). Lines represent the means of 5 to 10 mice per time point from at
650 least two independent experiments. Dashed line shows detection level of LGTV. a.u.,
651 arbitrary units.
652
653 **Figure 4. Identification of LGTV-infected cells.**
654 IFNAR$^{-/-}$ mice were infected intraperitoneally with 10^2 pfu LGTV and sacrificed at the
655 indicated time points post-infection. A, H&E staining of spleens of uninfected and LGTV
656 infected mice 4 days post-infection. Scale bar represents 50 µm. B, Sorting strategy of CD3$^+$,
657 B220$^+$, CD11c$^+$ and F4/80$^+$ cells. C, Splenocytes were isolated, stained for cell-specific
658 markers and sorted for F4/80$^+$, CD11c$^+$, B220$^+$ and CD3$^+$ cells. Viral load was measured by
659 real-time RT-PCR. Lines represent means of 4-5 samples from at least two independent
660 experiments. Dashed line shows detection level of LGTV. a.u., arbitrary units.
661
662 **Figure 5. Type I IFN response is essential in hematopoetic and non-hematopoetic cells**
663 **during LGTV infection.**
664 WT and IFNAR$^{-/-}$ mice were lethally irradiated and reconstituted with bone marrow from
665 IFNAR$^{-/-}$ or WT mice, respectively. After 6-8 weeks, chimeric mice were inoculated

intraperitoneally with 10^2 pfu LGTV. A, Survival was monitored and plotted as Kaplan-Meier curves (n=5-11). Data are cumulative of two independent experiments. Survival differences were tested for statistical significance by the log-rank test. B, Viral load was measured by real-time RT-PCR in spleen and lung, spinal cord and brain on day 2 and 4 post-infection. Lines represent the means of 5 mice per time point from two independent experiments. Dashed line shows detection level of LGTV. a.u., arbitrary units. Asterisks indicate values that were statistically significant: * P<0.05, ** P<0.01, *** P<0.0005, **** P<0.0001, based on the unpaired t-test.

Figure 6 Peripheral and local type I IFN response in the CNS is critical for survival of LGTV infection

A, Survival analysis of WT and IFNAR$^{-/-}$ mice after intracranial injection of 10 and 10^2 pfu of LGTV (n=5). B, Mice expressing a conditional IFNAR (IFNAR$^{fl/fl}$) were intercrossed with CreERT$^{+/-}$ mice to obtain mice with a deletion of IFNAR in the periphery (IFNAR$^{fl/fl}$CreERT$^{+/-}$). Mice were fed with tamoxifen and screened for tissue-specific deletion of exon 10 by PCR. PCR amplification of genomic DNA from IFNAR$^{fl/fl}$CreERT$^{+/-}$ mice resulted in a 339 bp fragment in cases Exon 10 was deleted. Li, liver, Lu, lung, S, spleen, BS, brain stem, OB, olfactory bulb, C, cerebrum, +, positive control, -, water control. Survival analysis of IFNAR$^{fl/fl}$ (n=9), IFNAR$^{-/-}$ (n=16), IFNAR$^{fl/fl}$CreERT$^{+/-}$ (n=5) and IFNAR$^{fl/fl}$NesCre$^{+/-}$ (n=13) mice after intraperitoneal infection with 10^2 pfu of LGTV. Mortality was followed for 21 days. Survival differences were tested for statistical significance by the log-rank test. C, IFNAR$^{fl/fl}$CreERT$^{+/-}$ and IFNAR$^{fl/fl}$NesCre$^{+/-}$ mice were infected intraperitoneally with 10^2 pfu of LGTV and viral load was measured by real-time RT-PCR in lung and brain on day 4 and 8 post-infection. Lines represent the means of 3-6

690 mice per time point from at least two independent experiments. Dashed line shows detection
691 level of LGTV. a.u., arbitrary units.
692
693 **Figure 7 Inflammatory responses in the brain upon LGTV infection**
694 WT and IFNAR$^{-/-}$ mice were infected intraperioneally with 10^2 pfu LGTV and analyzed 4
695 days post-infection. A, Immunohistochemical staining of LGTV E-protein (brown) in
696 different parts of the brain of IFNAR$^{-/-}$ mice. Scale bar represents 25 µm. B,
697 Immunohistochemical analysis of LGTV E- or NS5-protein expressing cells in the medulla
698 oblongata in IFNAR$^{-/-}$ mice. EP: E-protein of LGTV (brown), NS5: non-structural protein 5
699 of LGTV (brown), IBA1: microglia (red), GFAP: astrocytes (red), NeuN: neurons (red). Scale
700 bar represents 25 µm. C, Leukocytes infiltration into the CNS (n=5) was assessed by flow
701 cytometry at day 4 post-infection. Cells recovered from perfused brains were stained with
702 antibodies to CD11c, CD3, CD45 and CD11b. Total cell numbers were assessed by flow
703 cytometry. DC, dendritic cells, T, T cells, Mono, mononucleated cells, Mig, microglia. D,
704 Immunohistochemical analysis of microglia (IBA1: red) in the brain of uninfected and
705 infected IFNAR$^{-/-}$ mice. Scale bar represents 25 µm. E, Expression of proinflammatory
706 cytokines IL-6 and TNFα in the brains of WT and IFNAR$^{-/-}$ mice by real-time RT-PCR. F,
707 Detection of BBB integrity in WT and IFNAR$^{-/-}$ mice upon LGTV infection (n=4). Brains of
708 infected mice were isolated 4 days post-infection. One hour before harvesting, mice were
709 injected intravenously with Evans blue dye. Representative photographs are of the dorsal
710 surface. Quantification of Evans blue concentration in brain extracts. Data represent the mean
711 ± SEM and are cumulative from at least two independent experiments. Asterisks indicate
712 values that were statistically significant: *, $P < 0.05$, compared to WT mice, based on the
713 Mann-Whitney test.
714
715 **Figure 8. Type I IFN response prolongs survival of TBEV infections**

716 Survival analysis of WT and IFNAR$^{-/-}$ mice (n=5) after intraperitoneal infection with 10^4 pfu
717 of TBEV strain Hypr. Survival differences were tested for statistical significance by the log-
718 rank test.

Figure 1

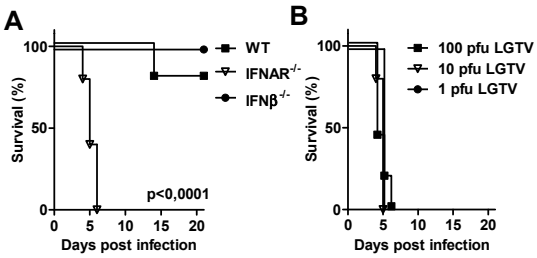

Figure 2

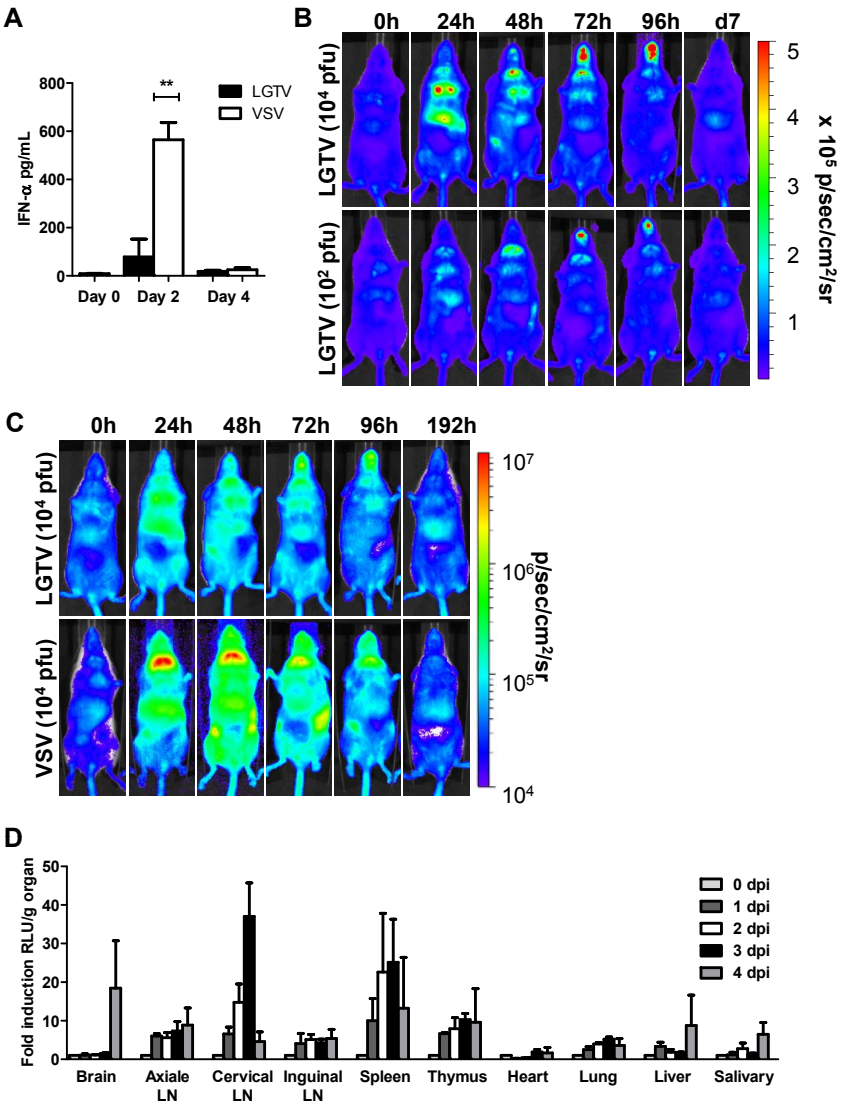

Figure 3

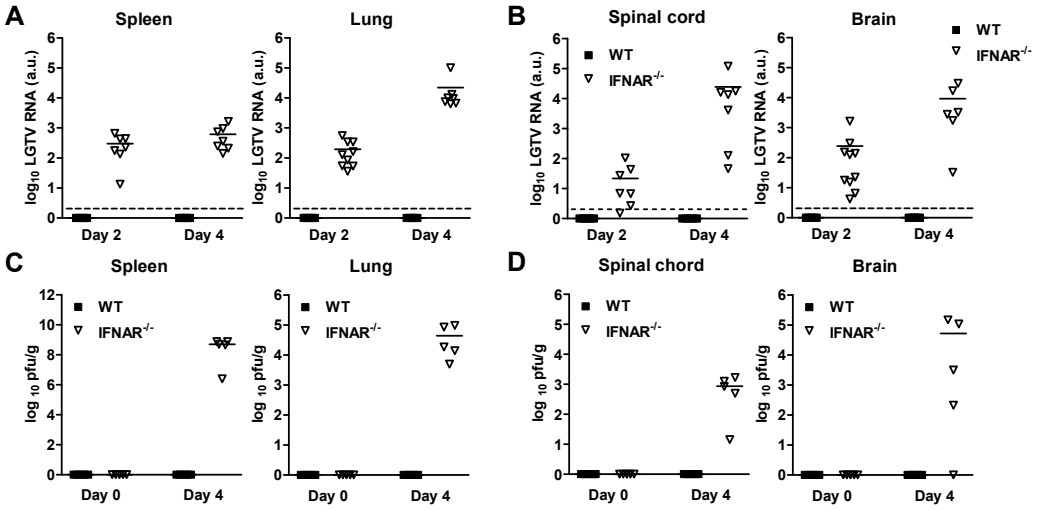

Figure 4

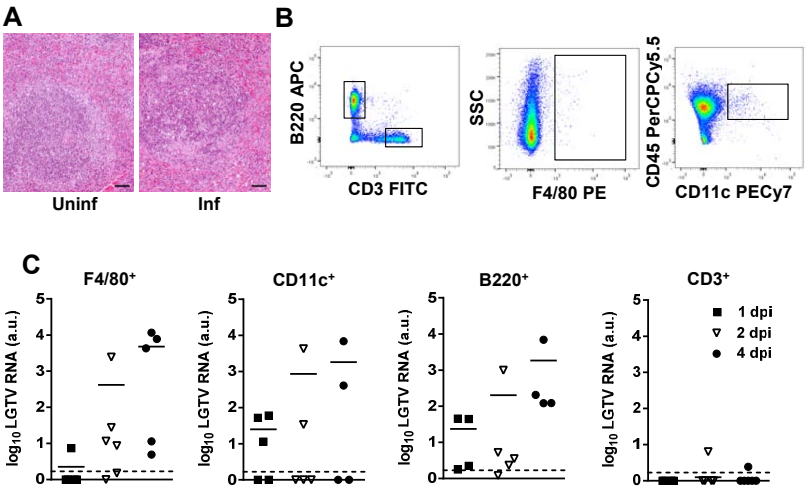

Figure 5

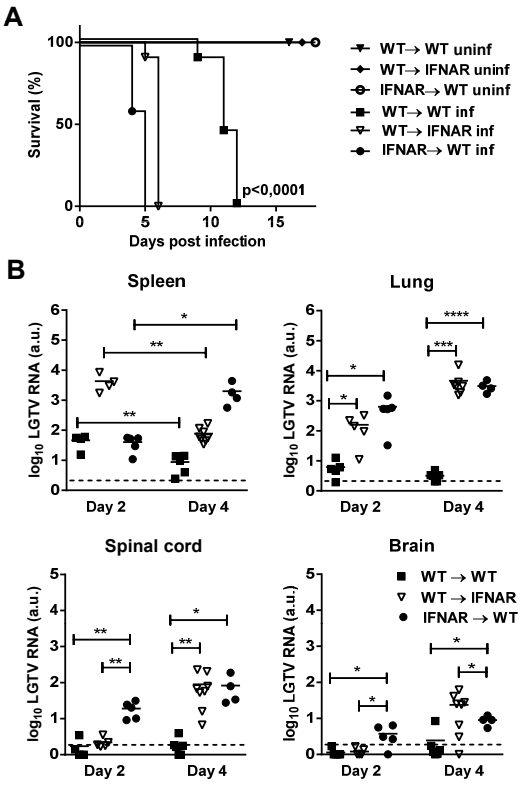

Figure 6

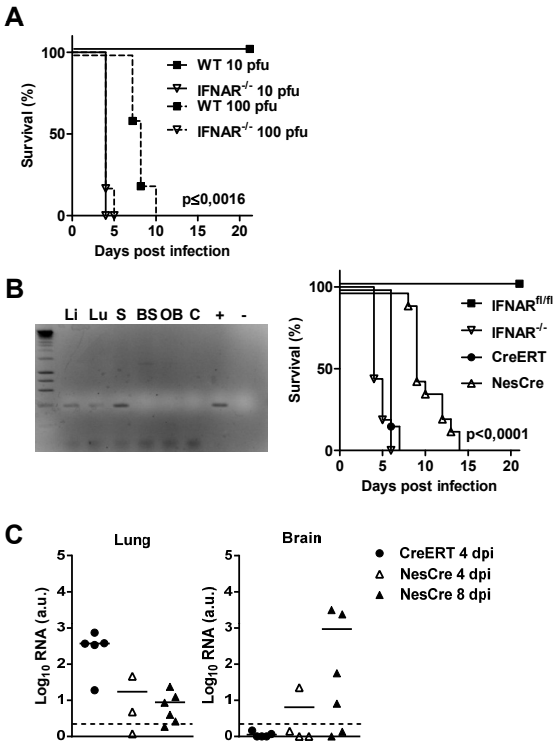

Figure 7

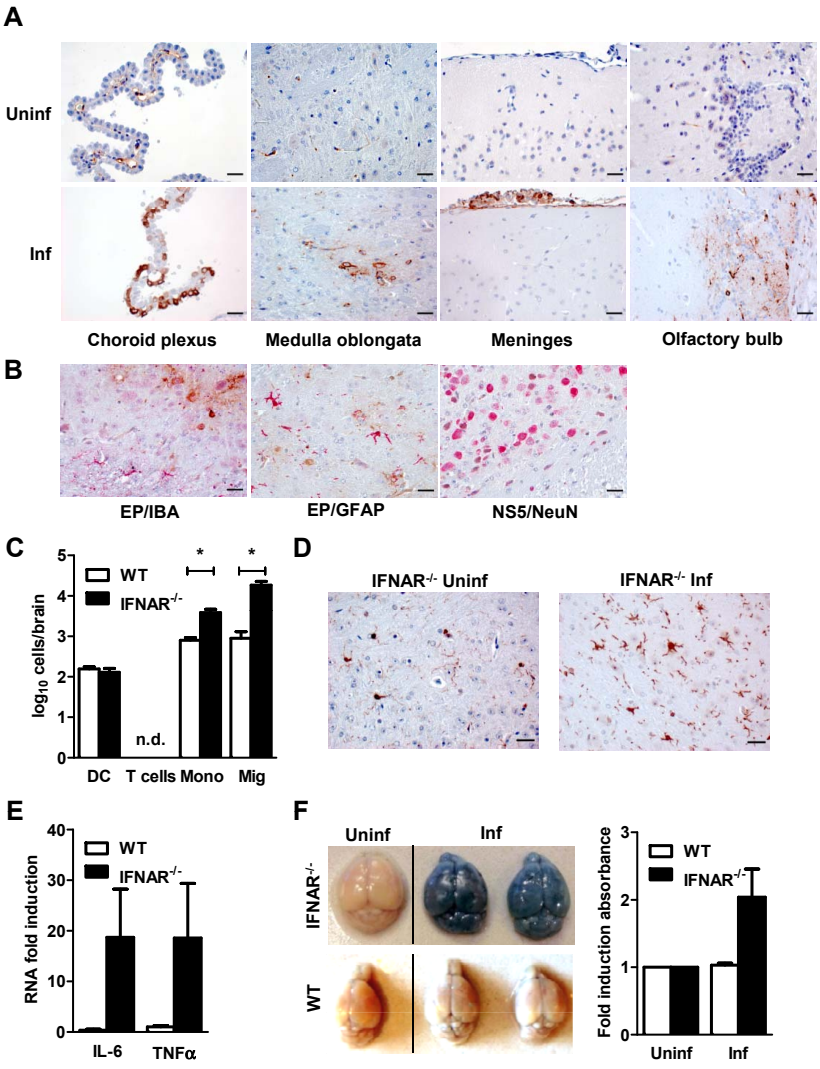

Figure 8